JOURNAL OF MATERIALS SCIENCE **39** (2004) 1185– 1193

Input error sensitivity of hardness and elastic modulus evaluated from indentation load-displacement records by Oliver and Pharr method

L. PRCHLIK
Department of Materials Science and Technology, Massachusetts Institute of Technology, Cambridge, MA 02139, USA
E-mail: lubos.prchlik@skoda.cz

Due to its straightforwardness and the ease of implementation the Oliver-Pharr method [1] has been used in the analysis of load-displacement records for more than a decade now. This paper provides analytical expressions relating the errors in the hardness and elastic modulus obtained by this method to systematic calibration errors of measured depth, force and frame compliance for spherical and sharp indentation. While in systems with zero frame compliance the sensitivity ratios for depth and force measurement were found to be constant, in systems with a finite frame compliance the error sensitivity changes with the absolute values of applied force and measured depth. The analytical predictions are compared with the true variation in derived materials parameters and the ranges of validity of the expressions are established. The error sensitivity with respect to different input variables and its implications for the actual measurement are discussed.

1. Introduction

The need to determine mechanical properties from small material volumes has driven the rapid development of depth-sensing indentation techniques—both with respect to testing equipment and analysis methods. Depth-sensing indentation is currently evolving from a research tool to a technique used in an ever expanding variety of scientific and industrial applications. For a specific depth sensing indentation system, its design concept represents a trade-off between the system price, robustness and its accuracy. Calibration errors may cause systematic errors in the measurement of the basic variables as illustrated by Fig. 1. Through the evaluation method applied, errors in measured input variables translate into errors in determined material characteristics.

Even though recent evaluation methods generate more complete sets of elastic-plastic parameters [2–7], the method proposed by Oliver and Pharr is still widely used and referred to [1, 8]. The method is based on the fundamental principles of contact mechanics [9, 10] rather than numerical calculations, and can be applied in principle to any indenter geometry. To the authror's knowledge, the most complete work treating various sources of error in sharp depth-sensing indentation evaluated by Oliver and Pharr method was that of Mencik *et al*. [11]. Mencik considered the effects of errors in the machine compliance and in measured variables separately, but explicit formulas relating the errors in machine compliance, calibration errors of depth/force to resulting errors in measured characteristics were not given.

The present study provides explicit estimates of output errors as a function of errors in measured input variables and verifies the derived *sensitivity coefficients* with specific examples for various indenter geometries and material parameters.

2. Sensitivity to measurement error

The Oliver and Pharr method derives elastic modulus and hardness from three main parameters of a load-displacement record: maximum depth, $h_{\max}$, maximum force, $F_{\max}$ and unloading slope, $(\mathrm{d}F/\mathrm{d}h)_{\max}$. Using the notation $F' \equiv (\mathrm{d}F/\mathrm{d}h)_{\max}$, governing relationships of the Oliver and Pharr method can be written as

$$H = \frac{F_{\max}}{A_{\text{contact}}^{\max}}, \tag{1}$$

$$E^* = \frac{\sqrt{\pi}}{2}\frac{F'}{\sqrt{A_{\text{contact}}^{\max}}}, \tag{2}$$

$$h_{\text{contact}}^{\max} = h_{\max} - 0.75\frac{F_{\max}}{F'}, \tag{3}$$

where A_{contact} stands for the projected contact area, H is the hardness (average pressure) and h_{contact} is the estimate of the vertical distance between the tip of the

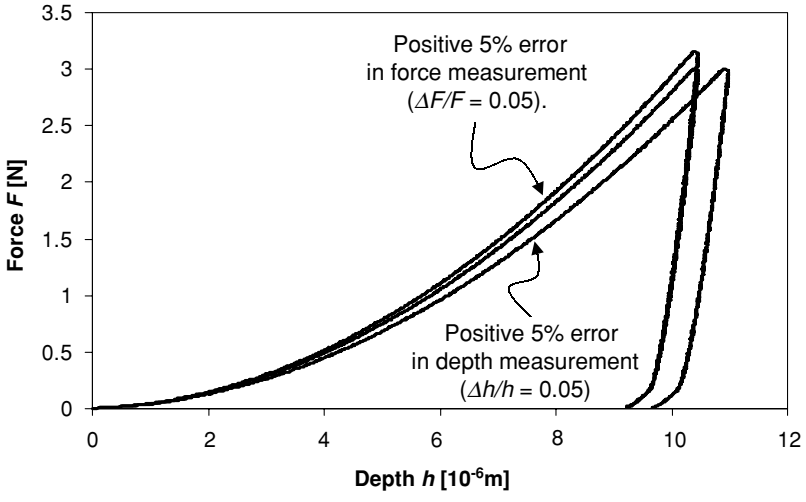

Figure 1 Load-displacement record for Aluminum alloy 6061 obtained with a Berkovich indenter. The plot shows the original data and data with +5% error in measured force and displacement, respectively.

indenter and the horizontal plane determined by the contact perimeter. E^* is the so called reduced elastic modulus that is determined from the elastic modulus and Poisson's ratio of the indenter and the sample material [1,10]:

$$E^* = \left[\frac{1-\nu_{\text{indenter}}^2}{E_{\text{indenter}}} + \frac{1-\nu_{\text{sample}}^2}{E_{\text{sample}}}\right]^{-1}. \tag{4}$$

The relationship between the contact depth, h_{contact}, and the contact area, A_{contact}, is required to complete the set of the Equations 1–3. For a spherical probe under conditions of the small indentation depth ($h_{\text{contact}} \ll R$) this relationship is

$$A_{\text{contact}} \cong 2\pi R h_{\text{contact}}. \tag{5}$$

For an ideally sharp Vickers or Berkovich indenter, the tip area function is

$$A_{\text{contact}} = 24.5 h_{\text{contact}}^2. \tag{6}$$

3. Error sensitivity of Young's modulus measurement

For spherical indentation, the elastic modulus can be expressed in the basic parameters $h_{\max}$, $F_{\max}$ and F' from Equations 2, 3 and 5 as

$$E^*_{\text{spherical}} = \frac{1}{2\sqrt{2R}} \frac{F'}{\sqrt{h_{\max} - 0.75\frac{F_{\max}}{F'}}}. \tag{7}$$

For Berkovich and Vickers indentation an equivalent relationship can be written as

$$E^*_{\text{sharp}} = \frac{1}{2}\sqrt{\frac{\pi}{24.5}} \frac{F'}{\left(h_{\max} - 0.75\frac{F_{\max}}{F'}\right)}. \tag{8}$$

In the following analysis, systematic measurement errors are treated. It is assumed that at each point of the load-displacement curve F-h, the relative errors of both measured variables F and h are constant as schematically depicted in Fig. 1. Relative errors are denoted as $(\frac{\Delta F}{F})$ and $(\frac{\Delta h}{h})$ for force and penetration depth, respectively. Such systematic errors are typically the result of the offset in the force and depth calibrations.

Assuming the errors of contact load and penetration depth are independent, the error of the reduced elastic modulus $\frac{\Delta E^*}{E^*}$ can be expressed as a function of the relative errors of both variables [12]:

$$\frac{\Delta E^*}{E^*} = \frac{1}{E^*}\left[\frac{\partial E^*}{\partial h}\left(\frac{\Delta h}{h}\right)h + \frac{\partial E^*}{\partial F}\left(\frac{\Delta F}{F}\right)F\right]_{\max}. \tag{9}$$

The reduced elastic modulus $E*$ is an implicit function of h and F:

$$E^* = E^*(h, F) = E^*[h_{\max}(h), F'(h, F), F_{\max}(F)]. \tag{10}$$

Therefore, combining Equations 9 and 10 the relative error of the elastic modulus can be written as

$$\begin{aligned}\frac{\Delta E^*}{E^*} &= \left[\left(\frac{\partial E^*}{\partial h_{\max}}\frac{\partial h_{\max}}{\partial h} + \frac{\partial E^*}{\partial F'}\frac{\partial F'}{\partial h}\right)_{\max}\frac{h_{\max}}{E^*}\right] \\ &\quad\times\left(\frac{\Delta h}{h}\right) + \left[\left(\frac{\partial E^*}{\partial F'}\frac{\partial F'}{\partial F} + \frac{\partial E^*}{\partial F_{\max}}\frac{\partial F_{\max}}{\partial F}\right)_{\max}\right. \\ &\quad\left.\times\frac{F_{\max}}{E^*}\right]\left(\frac{\Delta F}{F}\right).\end{aligned} \tag{11}$$

Equation 11 represents the overall relative error of the reduced elastic modulus as the function of relative errors in the measured penetration depth and contact force. The derivatives with respect to the parameters h and F (i.e., $\frac{\partial}{\partial h}$, $\frac{\partial}{\partial F}$) represent the change of the differentiated variable resulting from the uniform change of measured depth h or measured force F over their entire ranges (0, $h_{\max}$) and (0, $F_{\max}$), respectively. The

subscript 'max' denotes that all the derivatives are evaluated at the point of the maximum penetration depth and force ($h_{\max}$, $F_{\max}$). For simplicity, the subscript 'max' is dropped and it is understood that all the following derivatives are evaluated at the point ($h_{\max}$, $F_{\max}$).

Due to the assumed direct proportionality between parameters $h_{\max}$ and h as well as $F_{\max}$ and F, the derivatives $\frac{\partial h_{\max}}{\partial h}$ and $\frac{\partial F_{\max}}{\partial F}$ equal to one. Under the assumption of constant relative error over the entire depth and load ranges, the relative change in the unloading slope F' is proportional to the relative change in the force: $\frac{\partial F'}{\partial F}\frac{F_{\max}}{F'} = 1$. At the same time, the change in the unloading slope is inversely proportional to the relative change of the contact force, which leads to $\frac{\partial F'}{\partial h}\frac{h_{\max}}{F'} = -1$. Equation (11) can be therefore further simplified:

$$\frac{\Delta E^*}{E^*} = \left[\left(\frac{\partial E^*}{\partial h_{\max}} - \frac{\partial E^*}{\partial F'}\frac{F'}{h_{\max}}\right)\frac{h_{\max}}{E^*}\right]\left(\frac{\Delta h}{h}\right) + \left[\left(\frac{\partial E^*}{\partial F'}\frac{F'}{F_{\max}} + \frac{\partial E^*}{\partial F_{\max}}\right)\frac{F_{\max}}{E^*}\right]\left(\frac{\Delta F}{F}\right). \tag{12}$$

Equation 12 contains partial derivatives that need to be calculated based on Equations 7 and 8 for spherical and sharp indenters, respectively.

For spherical indentation, the derivative of the expression (7) with respect to F' yields

$$\frac{\partial E^*_{\text{spherical}}}{\partial F'} = \frac{1}{2\sqrt{2Rh_{\text{contact}}}}\left(1 - \frac{0.375F_{\max}}{F'h_{\text{contact}}}\right), \tag{13}$$

which can be rewritten as

$$\frac{\partial E^*_{\text{spherical}}}{\partial F'}\frac{F'}{E^*} = 1 - \frac{0.375F_{\max}}{F'h_{\text{contact}}} = 1 - 0.375\pi\frac{R}{a_{\text{contact}}}\frac{H_{\text{spherical}}}{E^*}. \tag{14}$$

The right hand side of Equation 14 has limits of 0.5 for a fully elastic case and 1 for materials with a low hardness to elastic modulus ratio.

Using a similar approach, the derivative can be taken with respect to $h_{\max}$, which leads to

$$\frac{\partial E^*_{\text{spherical}}}{\partial h_{\max}}\frac{1}{E^*} = -\frac{1}{2h_{\text{contact}}}. \tag{15}$$

For sharp indentation equations equivalent to expressions (14) and (15) are:

$$\frac{\partial E^*_{\text{sharp}}}{\partial F'}\frac{F'}{E^*} = 1 - 0.75\frac{F_{\max}}{F'h_{\text{contact}}} = 1 - 0.375\sqrt{24.5\pi}\frac{H_{\text{sharp}}}{E^*}, \tag{16}$$

$$\frac{\partial E^*_{\text{sharp}}}{\partial h_{\max}}\frac{1}{E^*} = -\frac{1}{h_{\text{contact}}}. \tag{17}$$

Taking the derivative of Equation 7 with respect to $F_{\max}$ and using Equation 13 for spherical indentation, it can be shown that

$$\left(\frac{\partial E^*_{\text{spherical}}}{\partial F'}\frac{F'}{F_{\max}} + \frac{\partial E^*}{\partial F_{\max}}\right)\frac{F_{\max}}{E^*} = 1 \tag{18}$$

Using Equations 8 and 16, the equality 18 can be proven valid for a sharp indenter as well (with $E^*_{\text{spherical}}$ replaced by E^*_{sharp}).

Finally, the overall sensitivity of the elastic modulus with respect to the measurement errors can be written using *sensitivity coefficients* K_{Eh} and K_{EF} as

$$\frac{\Delta E^*}{E^*} = -K_{\text{Eh}}\left(\frac{\Delta h}{h}\right) + K_{\text{EF}}\left(\frac{\Delta F}{F}\right). \tag{19}$$

The sensitivity coefficients are equal to the expressions in brackets from Equation 11. They can be explicitly calculated using Equations 14, 15, 18 and 16, 17, 18 for spherical and sharp indenters, respectively. The value of the coefficient K_{Eh} is 1.5 for spherical and 2 for sharp indentation, respectively. The coefficient K_{EF} has the value of 1 for both indenter shapes.

4. Error sensitivity of hardness measurement

The error sensitivity for hardness can be estimated using a similar approach. Hardness is calculated for the spherical and sharp indentation as

$$H_{\text{spherical}} = \frac{1}{2\pi R}\frac{F_{\max}}{\left(h_{\max} - 0.75\frac{F_{\max}}{F'}\right)} \tag{20}$$

and

$$H_{\text{sharp}} = \frac{1}{24.5}\frac{F_{\max}}{\left(h_{\max} - 0.75\frac{F_{\max}}{F'}\right)^2}, \tag{21}$$

respectively.

For hardness, an expression similar to Equation 12 for elastic modulus can be written as

$$\frac{\Delta H}{E} = \left[\left(\frac{\partial H}{\partial h_{\max}} - \frac{\partial H}{\partial F'}\frac{F'}{h_{\max}}\right)\frac{h_{\max}}{H}\right]\left(\frac{\Delta h}{h}\right) + \left[\left(\frac{\partial H}{\partial F'}\frac{F'}{F_{\max}} + \frac{\partial H}{\partial F_{\max}}\right)\frac{F_{\max}}{H}\right]\left(\frac{\Delta F}{F}\right). \tag{22}$$

The derivatives with respect to $h_{\max}$ and F' can be expressed for spherical indentation as

$$\frac{\partial H_{\text{spherical}}}{\partial h_{\max}}\frac{1}{H_{\text{spherical}}} = -\frac{1}{h_{\text{contact}}},$$

and

$$\frac{\partial H_{\text{spherical}}}{\partial F'}\frac{F'}{H_{\text{spherical}}} = -\frac{0.75F_{\max}}{F'h_{\text{contact}}}. \tag{23}$$

Similarly for sharp indentation, the derivations with respect to F' and h_{max} yield

$$\frac{\partial H_{sharp}}{\partial h_{max}}\frac{1}{H_{sharp}} = -\frac{2}{h_{contact}},$$

and

$$\frac{\partial H_{sharp}}{\partial F'}\frac{F'}{H_{sharp}} = -\frac{1.5F_{max}}{F'h_{contact}}. \quad (24)$$

The following expression is valid for both spherical and sharp indentation:

$$\left(\frac{\partial H}{\partial F'}\frac{F'}{F_{max}} + \frac{\partial H}{\partial F_{max}}\right)\frac{F_{max}}{H} = 1. \quad (25)$$

The overall sensitivity of the evaluation of hardness is now:

$$\frac{\Delta H}{H} = -K_{Hh}\left(\frac{\Delta h}{h}\right) + K_{HF}\left(\frac{\Delta F}{F}\right) \quad (26)$$

The value of the coefficient K_{Hh} is 1 for spherical and 2 for sharp indenters. The coefficient K_{HF} has a value of 1 for both indenter shapes.

It can be easily shown that the expressions for sharp indentation derived here for the specific area function ($A = 24.5h^2$) apply to any self-similar indenter for which $A \propto h^2$.

5. Error sensitivity in systems with finite frame compliance

In the majority of depth-sensing systems, the displacement sensor is placed serially with other mechanical elements having compliances comparable to the contact compliance of the indenter-material contact. The net displacement h of the indentation contact is then obtained by subtracting an additional displacement caused by the frame compliance C_f from the total measured displacement h^{meas}:

$$h = h^{meas} - C_f F \quad \text{and} \quad h_{max} = h^{meas}_{max} - C_f F_{max}. \quad (27)$$

The accuracy of the depth measurement depends on the calibration of two variables—measured depth h^{meas} and the frame compliance C_f. In this configuration, h^{meas} rather than h displays a constant relative error over the entire measurement range ($\Delta h^{meas}/h^{meas}$). The elastic modulus is now expressed as the function of three variables h^{meas}, F and C_f:

$$\begin{aligned} E^* &= E^*(h^{meas}, F, C_f) \\ &= E^*[h_{max}(h^{meas}, C_f), F'(h^{meas}, F, C_f), F_{max}(F)] \end{aligned} \quad (28)$$

An equivalent of Equation 12 can be written as

$$\begin{aligned} \frac{\Delta E}{E^*} &= \left(\frac{\partial E}{\partial h_{max}}\frac{\partial h_{max}}{\partial h^{meas}}\frac{h^{meas}}{E^*} + \frac{\partial E}{\partial F'}\frac{\partial F'}{\partial h^{meas}}\frac{h^{meas}}{E^*}\right) \\ &\times \left(\frac{\Delta h^{meas}}{h^{meas}}\right) + \left(\frac{\partial E^*}{\partial h_{max}}\frac{\partial h_{max}}{\partial C_f}\frac{C_f}{E^*} + \frac{\partial E^*}{\partial F'}\frac{\partial F'}{\partial C_f}\frac{C_f}{E^*}\right) \\ &\times \left(\frac{\Delta C_f}{C_f}\right) + \left(\frac{\partial E^*}{\partial F_{max}}\frac{\partial F_{max}}{\partial F}\frac{F_{max}}{E^*} + \frac{\partial E^*}{\partial F'}\frac{\partial F'}{\partial F}\frac{F_{max}}{E^*}\right) \\ &\times \left(\frac{\Delta F}{F}\right). \end{aligned} \quad (29)$$

In the case of hardness the error sensitivity is expressed as

$$\begin{aligned} \frac{\Delta H}{H} &= \left(\frac{\partial H}{\partial h_{max}}\frac{\partial h_{max}}{\partial h^{meas}}\frac{h^{meas}_{max}}{H} + \frac{\partial H}{\partial F'}\frac{\partial F'}{\partial h^{meas}}\frac{h^{meas}_{max}}{H}\right) \\ &\times \left(\frac{\Delta h^{meas}}{h^{meas}}\right) + \left(\frac{\partial H}{\partial h_{max}}\frac{\partial h_{max}}{\partial C_f}\frac{C_f}{H} + \frac{\partial H}{\partial F'}\frac{\partial F'}{\partial C_f}\frac{C_f}{H}\right) \\ &\times \left(\frac{\Delta C_f}{C_f}\right) + \left(\frac{\partial H}{\partial F_{max}}\frac{\partial F_{max}}{\partial F}\frac{F_{max}}{H} + \frac{\partial H}{\partial F'}\frac{\partial F'}{\partial F}\frac{F_{max}}{H}\right) \\ &\times \left(\frac{\Delta F}{F}\right). \end{aligned} \quad (30)$$

Using Equations 27 and considering that

$$F' = \lim_{\substack{F\to -F_{max}- \\ h^{meas}\to h^{meas}_{max}-}} \left(\frac{F_{max} - F}{\left(h^{meas}_{max} - C_f F_{max}\right) - \left(h^{meas} - C_f F\right)}\right),$$

the following derivatives can be calculated:

$$\begin{aligned} &\frac{\partial h_{max}}{\partial h^{meas}} = 1, \quad \frac{\partial h_{max}}{\partial C_f} = -F_{max}, \quad \frac{\partial F'}{\partial C_f} = (F')^2, \\ &\frac{\partial F'}{\partial F} = \frac{F'}{F_{max}}(1 + C_f F'), \\ &\frac{\partial F'}{\partial h^{meas}} = -\frac{F'}{h^{meas}}(1 + C_f F') \end{aligned} \quad (31)$$

Based on Equations 30–31 and expressions (13)–(17), the error sensitivity for the elastic modulus derived from the spherical and sharp indentation is expressed as

$$\frac{\Delta E^*}{E^*} = K_{Eh}\left(\frac{\Delta h^{meas}}{h^{meas}}\right) + K_{EF}\left(\frac{\Delta F}{F}\right) + K_{EC_f}\left(\frac{\Delta C_f}{C_f}\right) \quad (32)$$

with the sensitivity coefficients calculated as

$$K_{Eh} = -\alpha\frac{h^{meas}_{max}}{h_{contact}} - \left(1 - \alpha\frac{0.75F_{max}}{F'h_{contact}}\right)\left(1 + C_f F'\right),$$

$$K_{EF} = 1 + \alpha\frac{0.75F_{max}C_f}{h_{contact}} + C_f F',$$

and

$$K_{\mathrm{EC_f}} = \alpha \frac{F_{\max} C_{\mathrm{f}}}{h_{\mathrm{contact}}} + \left(1 - \alpha \frac{0.75 F_{\max}}{F' h_{\mathrm{contact}}}\right) F' C_{\mathrm{f}},$$

where α is 0.5 and 1 for spherical and sharp indenters, respectively.

Using the Equations 30–31 and expressions (23)–(24), the error sensitivity of hardness derived from the spherical and sharp indentation is

$$\frac{\Delta H}{H} = K_{\mathrm{Hh}} \left(\frac{\Delta h^{\mathrm{meas}}}{h^{\mathrm{meas}}}\right) + K_{\mathrm{HF}} \left(\frac{\Delta F}{F}\right) + K_{\mathrm{HC_f}} \left(\frac{\Delta C_{\mathrm{f}}}{C_{\mathrm{f}}}\right) \tag{33}$$

with

$$K_{\mathrm{Hh}} = \alpha \left[-2 \frac{h_{\max}^{\mathrm{meas}}}{h_{\mathrm{contact}}} + \frac{1.5 F_{\max}}{F' h_{\mathrm{contact}}} \left(1 + C_{\mathrm{f}} F'\right)\right],$$

$$K_{\mathrm{HF}} = 1 + \alpha \frac{1.5 F_{\max} C_{\mathrm{f}}}{h_{\mathrm{contact}}},$$

and

$$K_{\mathrm{HC_f}} = \alpha \frac{F_{\max} C_{\mathrm{f}}}{2 h_{\mathrm{contact}}}.$$

The coefficent α in Equation 33 has again value of 0.5 and 1 for spherical and sharp indentation, respectively. The expressions (32), (33) reduce to the Equations 19 and 26 for the $C_{\mathrm{f}} \to 0$ (i.e., $h^{\mathrm{meas}} \to h$ and $(\Delta h^{\mathrm{measured}}/h^{\mathrm{measured}}) \to (\Delta h/h)$).

6. Verification and examples

In the following section, the derived expressions will be verified by comparing error predictions with actual variations in measured variables for several specific examples of indentation measurements. The comparison will be made for an ideally rigid frame as well as for a frame with a finite frame compliance.

7. Ideally rigid frame

Fig. 2 shows the variation of the elastic modulus and hardness for sharp indentation as a function of the error in the measured depth h in the range $\pm 15\%$. To render such comparison, the displacement of the original load-displacement record obtained with a spherical indenter (aluminum alloy 6061, indenter $R = 0.39$ mm, $h_{\max} = 10$ μm, $F_{\max} = 21.4$ μm) was multiplied by a set of appropriate constants and analyzed. The true variation is plotted as the set of points; while the predictions calculated from Equations 19 and 26 are plotted as solid lines ($K_{\mathrm{Eh}} = 1.5$, $K_{\mathrm{Hh}} = 1$, $K_{\mathrm{EF}} = K_{\mathrm{HF}} = 1$).

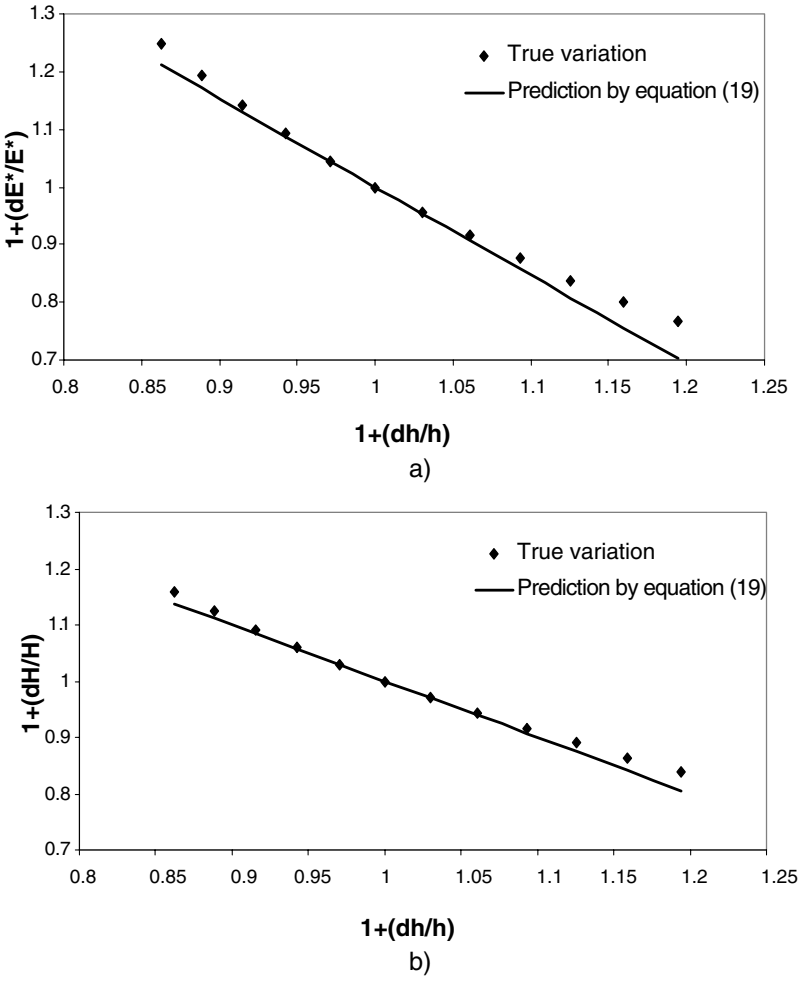

Figure 2 Relative errors of the reduced elastic modulus (a) and hardness (b) as the function of the relative error in contact depth for spherical indentation of Aluminum alloy 6061 on a tester with zero frame compliance ($R = 0.39$ mm, $F_{\max} = 21.4$ N, $h_{\max} = 10$ μm).

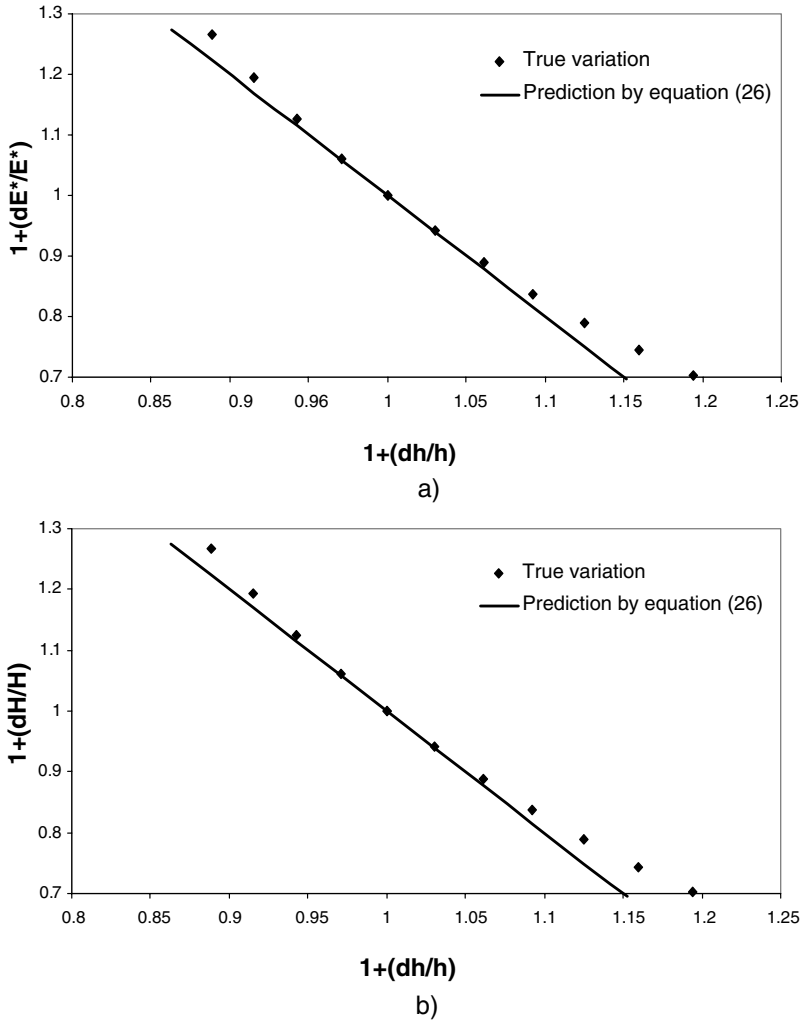

Figure 3 Relative errors of the reduced elastic modulus (a) and hardness (b) as a function of the relative error in contact depth for sharp indentation of Aluminum alloy 6061 on a tester with zero frame compliance (Berkovich indenter, $F_{max} = 3$ N, $h_{max} = 10.45$ μm).

Fig. 3 shows a similar comparison for sharp indentation. The prediction of the error in the parameters E^* and H for sharp indentation is based again on Equations 19 and 26 with sensitivity coefficients $K_{Eh} = K_{Hh} = 2$ and $K_{EF} = K_{HF} = 1$. Both for hardness and elastic modulus, the difference between the predicted and the actual variation is larger than in the case of the spherical indentation.

8. Finite frame compliance

Table I lists parameters of indentation records for two aluminum alloys obtained with sharp and spherical indenters. The original data were collected on a Nanotest 600 (Micromaterials, Wrexham, UK) with the nominal frame compliance of 0.5 μm/N. Calculated hardness, elastic modulus and corresponding error sensitivity coefficients are also listed in Table I. It can be seen that the sensitivity coefficients are significantly larger here compared to the case of the rigid frame ($C_f = 0$) discussed in the previous paragraph. Error sensitivity coefficients for hardness (K_{Hh}, K_{HF}, K_{HCf}) are smaller than the coefficients for elastic modulus ((K_{Eh}, K_{EF}, K_{ECf}), which was not the case for the zero frame compliance. The frame-compliance sensitivity coefficients K_{ECf} and K_{HCf} are lower than the

TABLE I Testing parameters, results and error sensitivity coefficients for aluminum alloys 6061 and 7075 tested with spherical and sharp indenters on a tester with a compliance 0.5 μm/N ($E^*_{6061} = 72$ GPa, $E^*_{7075} = 74$ GPa)

						Output parameters		Elastic modulus error sensitivity			Hardness error sensitivity		
Material	F_{max}	h_{max} (μm)	F' (μm/N)	$h_{contact}$ (μm)	$F'C_f$	E^* (GPa)	H (GPa)	K_{Eh}	K_{ECf}	K_{EF}	K_{Hh}	K_{HCf}	K_{HF}
Spherical indentation indenter $R = 0.39$ mm ($E_{WC\text{-}Co} = 618$ Gpa)													
Al 6061	21.4 N	10	13.6	8.8	6.73	81	0.99	−8.38	6.68	8.18	−1.3	0.3	1.9
Al 7075	15.1 N	5.5	9.06	4.24	4.53	78	1.44	−6.25	4.75	6.2	−1.45	0.45	2.34
Sharp indentation Berkovich indenter ($E_{Diamond} = 1141$ Gpa)													
Al 6061	3 N	10.45	4.72	9.98	2.48	89	1.18	−4.4	2.4	3.47	−2.08	0.08	1.22
Al 7075	9.7 N	15	6.8	9.98	3.4	88	2.08	−5.5	3.5	4.68	−2.18	0.18	1.53

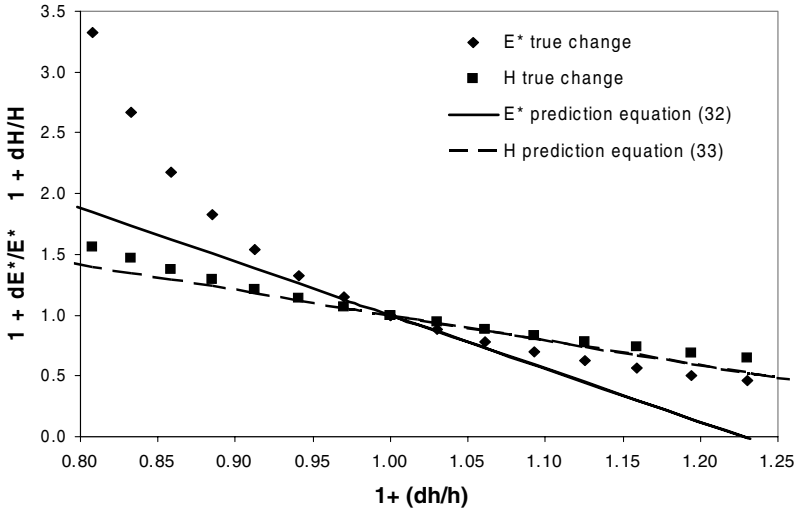

Figure 4 Relative errors of the reduced elastic modulus and hardness as a function of the relative error in contact depth for sharp indentation of Aluminum alloy 6061 on a tester with frame compliance $C_f = 0.5$ μm/N (Berkovich indenter, $F_{max} = 3$ N, $h_{max} = 10.45$ μm).

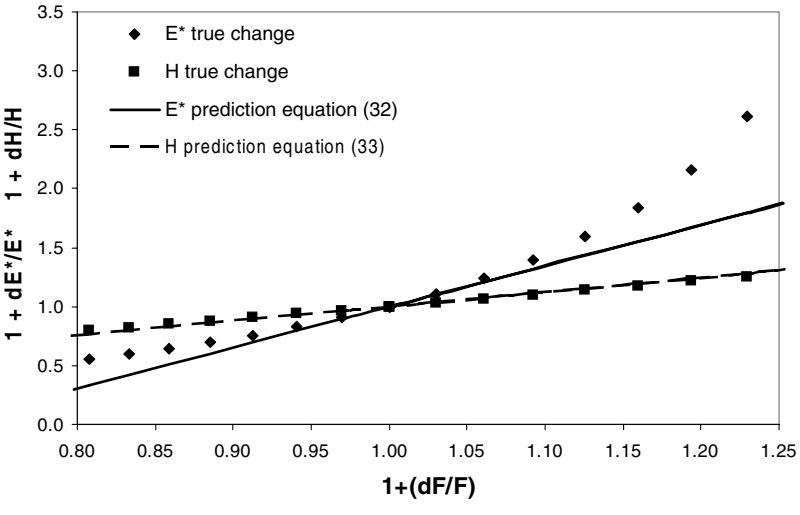

Figure 5 Relative errors of the reduced elastic modulus and hardness as a function of the relative error in applied force for sharp indentation of Aluminum alloy 6061 on a tester with frame compliance $C_f = 0.5$ μm/N (Berkovich indenter, $F_{max} = 3$ N, $h_{max} = 10.45$ μm).

coefficients K_{Eh}, K_{EF}, K_{Hh}, K_{HF} related to the measurement of penetration depth and force. In particular, for hardness, the method appears to be relatively insensitive to the accuracy of the calibration of the frame compliance.

Figs 4, 5, and 6 compare estimated and true errors with respect to calibration errors of all three inputs—h, F and C_f. The curve for aluminum alloy 6061 loaded with a Berkovich indenter to the maximum load of 3 N presented in Fig. 1 was used as a reference data set. There is a clear difference in the input error sensitivity of elastic modulus and hardness. The hardness variation resulting from the same change of a given input parameter is much smaller compared to the variation in the elastic modulus and follows a nearly linear trend with respect to a change in all three parameters h^{meas}, F, and C_f. The variation of elastic modulus is not only larger, but also shows a nonlinearity with respect to errors in all input parameters.

Fig. 7a shows the sensitivity coefficients K_{EF}, K_{ECf} normalized with respect to K_{Eh} plotted as the function of $F'C_f$. $F'C_f$ represents the ratio of the machine compliance and the contact sample compliance (i.e., C_f/C_{sample}) Fig. 7b presents a similar plot for the coefficients K_{HF}, K_{HCf} normalized with respect to K_{Hh}. The plots in Fig. 7 are again based on the load-displacement data from the sharp indentation of the aluminum alloy 6061 presented in Fig. 1. The frame compliance was varied from 0 to 0.7 μm/N. Both charts of Fig. 7 illustrate how the analysis becomes more sensitive to force measurement with increasing $F'C_f$.

At this point one could conclude and rewrite the Equations 32, 33 into the form of an expression relating the standard deviation of the calculated parameters to the standard deviations in the calibration of the total depth, force and frame compliance. Such an expression would have the following form for the elastic modulus [12]:

$$\frac{\sigma(E^*)}{E^*} = \left[\left(K_{Eh}\frac{\sigma(h^{meas})}{h^{meas}}\right)^2 + \left(K_{EC_f}\frac{\sigma(C_f)}{C_f}\right)^2 + \left(K_{EF}\frac{\sigma(F)}{F}\right)^2\right]^{0.5} \quad (34)$$

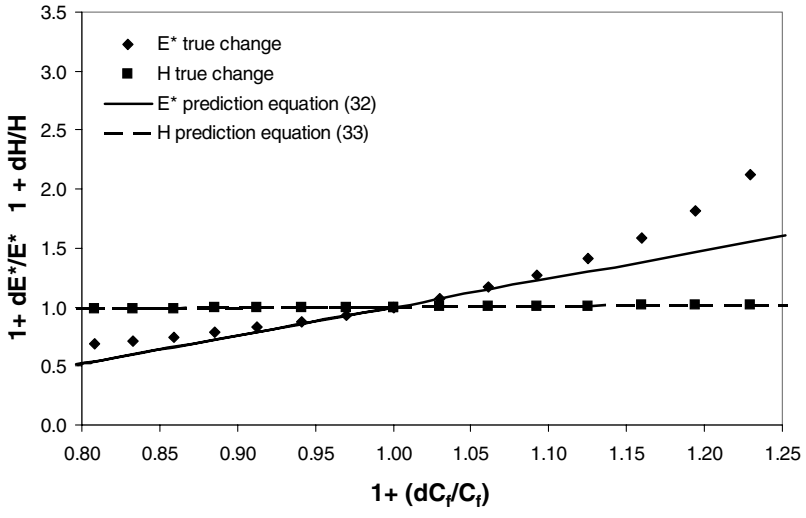

Figure 6 Relative errors of the reduced elastic modulus and hardness as a function of the relative error in frame compliance for sharp indentation of Aluminum alloy 6061 on a tester with nominal frame compliance $C_f = 0.5$ μm/N (Berkovich indenter, $F_{max} = 3$ N, $h_{max} = 10.45$ μm).

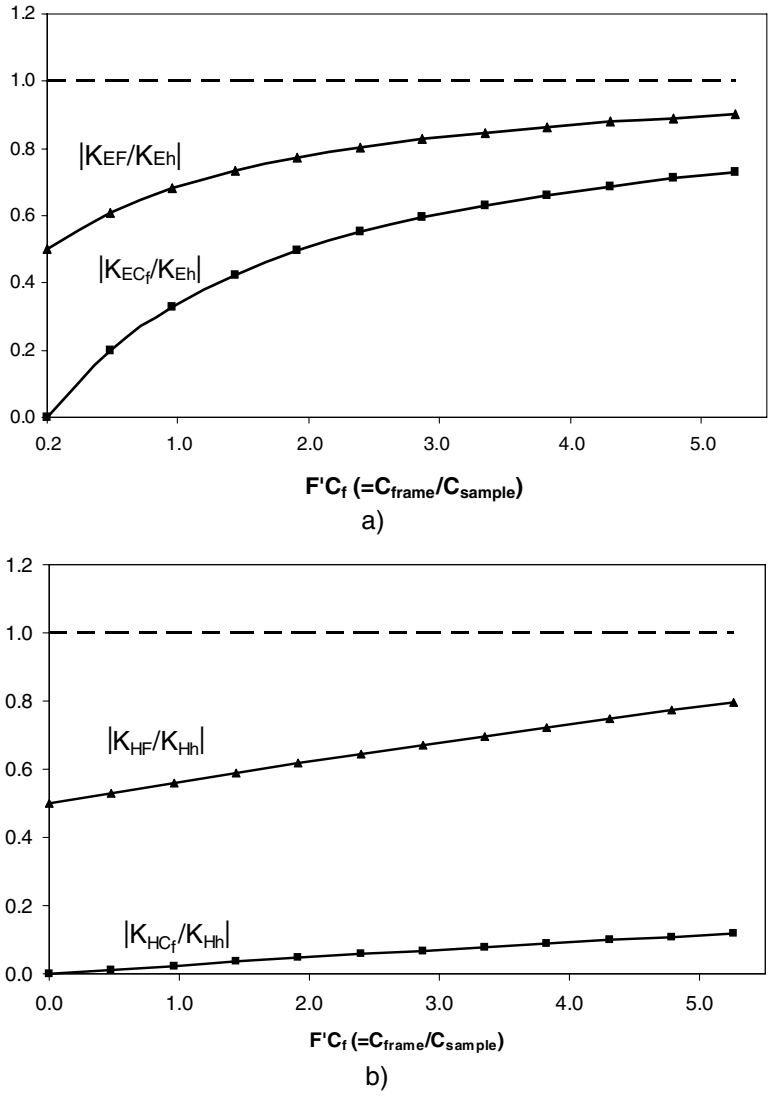

Figure 7 (a) Error sensitivity ratios K_{Eh}, K_{ECf} normalized with respect to K_{Eh} and (b) error sensitivity ratios K_{Hh}, K_{HCf} normalized with respect to K_{Hh}. $F'C_f$ represents the relative ratio of the frame compliance to the contact sample compliance (Berkovich indentation of aluminum alloy 7075, $F_{max} = 9.7$ N, $h_{max} = 15$ μm).

The expression (34) is based on the assumption of the independent calibration of all three variables. The independence of the calibration of the contact depth and force is satisfied in the majority of the depth sensing systems, but the calibration of the compliance is usually based on previously conducted depth and force calibrations. Thus, a calibration overestimating the force measurement will lead to smaller value of the frame compliance, which will in return reduce the overall error, since the error sensitivities have opposite signs. The right side of the Equation 34 should contain negative covariation coefficients that are not explicitly known and depend on the approach used in the compliance calculation. Expression (34) therefore represents a conservative estimate of the measurement error. The actual average error in the measurement of the elastic modulus will be smaller as a consequence of the covariance between the compliance calibration and the depth/force calibrations.

9. Other sources of systematic error

This study has focused on errors introduced into the measurement as the result of systematic measurement calibration errors. Other significant errors introduced into the measurement of mechanical properties by indentation are errors originating from the pile-up of the material around the indenter. Several studies have been performed to numerically predict or experimentally measure the pile-up effects for both the spherical and sharp (Berkovich or conical indenter) indentation [13–16]. In addition to pile-up, roughness and tilt of sample surface may represent problems for an industrial application of the indentation technique. Tilt and surface undulations of the sample surface can cause variations in the pressure distribution and additional lateral forces to the indenter. This is especially critical in the initial stage of the contact for the spherical indenter, where the uncompensated lateral force may lead to a lateral sliding of the indenter.

10. Summary

This study presented analytical expressions relating the error in the calculated elastic modulus and indentation hardness, evaluated by the Oliver and Pharr method, to the systematic errors in the measured depth, force and frame compliance. Systems with ideally stiff frames and finite-stiffness frames were discussed. Equations 19, 26 and 32, 33 express systematic output errors as function of input errors for zero and finite frame compliance, respectively. The expressions were derived based on a first order Taylor expansion and estimate errors accurately in the vicinity of the nominal values of the measured variable. Within range of $\pm 10\%$ of input error, the estimated and actual errors were in a good agreement for all load-displacement records considered. The prediction agreed with the true variation in a wider range of hardness compared to elastic modulus. Since the second derivatives of error curves for both hardness and elastic modulus are positive, the linear expressions presented underestimate positive errors and overestimate negative output errors.

Acknowledgement

This work was supported by the MRSEC program of the National Science Foundation grant #DMR 0080021 to the Center for Thermal Spray Research at SUNY, Stony Brook and related sub-contact to MIT, Cambridge. Help and inputs from B. Moser, M. Dao and S. Sampath are gratefully acknowledged.

References

1. W. C. OLIVER and G. M. PHARR, *J. Mater. Res.* **7** (1992) 1564.
2. B. TALJAT, T. ZACHARIA and F. KOSEL, *Intern. J. Solids Struct.* **35** (1998) 4411.
3. M. DAO, N. CHOLLACOOP, K. J. VAN VLIET, T. A. VENKATESH and S. SURESH, *Acta Materialia* **49** (2001) 3899.
4. T. A. VENKATESH, K. J. VAN VLIET, A. E. GIANNAKOPOULOS and S. SURESH, *Scripta Materialia* **42** (2000) 833.
5. N. HUBER, D. MUNZ and C. TSAKMAKIS, *J. Mater. Res.* **12** (1997) 2459.
6. S. KUCHARSKI and Z. MROZ, *Mater. Sci. Engin. Struct. Mater. Proper. Microstr. Proc.* **318** (2001) 65.
7. S. KUCHARSKI and Z. MROZ, *J. Engin. Mater. Tech.-Trans. Asme* **123** (2001) 245.
8. A. C. FISCHER-CRIPPS, *Vacuum* **58** (2000) 569.
9. C. M. CHENG and Y. T. CHENG, *Appl. Phys. Lett.* **71** (1997) 2623.
10. G. M. PHARR, W. C. OLIVER and F. R. BROTZEN, *J. Mater. Res.* **7** (1992) 613.
11. J. MENCIK and M. V. SWAIN, *ibid.* 10 (1995) 1491.
12. A. A. CLIFFFORD, "Multivariate Error Analysis" (Halsted Press, New York, 1973).
13. B. TALJAT, T. ZACHARIA and G. M. PHARR, Pile-up Behavior of Spherical Indentations in Egineering Materials," in "Fundamentals of Nanoindentation and Nanotribology," Vol. 522, edited by N. R. Moody, W. W. Gerberich, N. Burgham and S. P. Baker (Materials Research Society, San Francisco, 1998) p. 33.
14. A. BOLSHAKOV and G. M. PHARR, *J. Mater. Res.* **13** (1998) 1049.
15. J. ALCALA, A. C. BARONE and M. ANGLADA, *Acta Materialia* **48** (2000) 3451.
16. J. R. MATTHEWS, *Acta Metallurgica* **28** (1980) 311.

Received 29 May
and accepted 13 October 2003